Self-Activation of Guanosine Triphosphatase Activity by Oligomerization of the Bacterial Cell Division Protein FtsZ†

Thomas M. Sossong, Jr.,*,‡ Michael R. Brigham-Burke,§ Preston Hensley,§,|| and Kenneth H. Pearce, Jr.*,‡,⊥

Department of Anti-Infectives Research, SmithKline Beecham Pharmaceuticals, 1250 South Collegeville Road, Collegeville, Pennsylvania 19426, and Department of Structural Biology, SmithKline Beecham Pharmaceuticals, 709 Swedeland Road, King of Prussia, Pennsylvania 19406

Received April 22, 1999; Revised Manuscript Received September 2, 1999

ABSTRACT: The essential bacterial cell division protein FtsZ (filamentation temperature-sensitive protein Z) is a distant homologue to the eukaryotic cytoskeletal protein tubulin. We have examined the GTP hydrolytic activity of *Escherichia coli* FtsZ using a real-time fluorescence assay that monitors phosphate production. The GTPase activity shows a dramatic, nonlinear dependence on FtsZ concentration, with activity only observed at enzyme concentrations greater than 1 μM. At 5 μM FtsZ, we have determined a K_m of 82 μM GTP and a V_{max} of 490 nmol of P_i min^{-1} (mg of protein)$^{-1}$. Hydrolysis of GTP requires Mg^{2+} and other divalent cations substitute only poorly for this requirement. We have compared the concentration dependence of FtsZ GTPase activity with the oligomeric state by use of analytical ultracentrifugation and chemical cross-linking. Equilibrium analytical ultracentrifugation experiments show that FtsZ exists as 68% dimer and 13% trimer at 2 μM total protein concentration. Chemical cross-linking of FtsZ also shows that monomer, dimer, trimer, and tetramer species are present at higher (>2 μM) FtsZ concentrations. However, as shown by analytical centrifugation, GDP-bound FtsZ is significantly shifted to the monomeric state, which suggests that GTP hydrolysis regulates polymer destabilization. We also monitored the effect of nucleotide and metal ion on the secondary structure of FtsZ; nucleotide yielded no evidence of structural changes in FtsZ, but both Mg^{2+} and Ca^{2+} had significant effects on secondary structure. Taken together, our results support the hypothesis that Mg^{2+}-dependent GTP hydrolysis by FtsZ requires oligomerization of FtsZ. On the basis of these results and structural comparisons with the $\alpha-\beta$ tubulin dimer, GTP is likely hydrolyzed in a shared active site formed between two monomer subunits.

For a bacterial cell to successfully divide, many events at the protein level must occur correctly and in the proper sequence (*1*). One of these processes is the specific localization of the protein FtsZ to the midpoint of the actively dividing bacterium. Several reports have directly demonstrated that FtsZ polymerizes into a ringlike structure at the midcell (*2*−*4*). One suggestion for the function of this Z-ring is that it may act mechanically, possibly in concert with other proteins, to power the invagination of the outer membrane, cell wall, and inner membrane. Another possible role is that FtsZ may simply serve as a structural scaffold that directs localization of other key cell division proteins. Regardless, FtsZ plays a central role in the bacterial cell cycle and its presence is absolutely required for cell viability.

The sequence of FtsZ is highly conserved throughout nearly all prokaryotes, including mycobacteria, archeae, and chloroplasts, and there is very limited [10−18% overall (*5*)] but significant sequence homology with eukaryotic tubulins. Like tubulin, FtsZ is a GTPase, and these two enzymes share a unique GTP-binding motif, GGGTG(ST)G. This sequence, known as the G-box, is distinct from motifs found in other well-known GTPases, such as $p21^{ras}$ and EF-Tu (*6*). Despite the lack of overall sequence similarity between FtsZ and tubulin, crystal structures of *Methanococcus jannaschii* FtsZ (*7*) and the $\alpha-\beta$ tubulin dimer (*8*) have recently shown that these proteins share a strikingly similar three-dimensional fold.

The GTPase activity of FtsZ has been loosely associated with its polymerization, and mutants of FtsZ lacking GTPase activity do not support cell division (*9*, *10*). In vitro experiments have shown that FtsZ forms polymers in the presence of GTP and that depolymerization occurs after exhaustion of GTP (*11*). Electron microscopy studies have visualized GTP-induced polymeric structures, but only by inclusion of stabilizing agents such as DEAE-dextran and Ca^{2+} (*12*−*14*). Even with this information, the precise molecular mechanism by which nucleotide modulates polymerization is not known. Additionally, the role of GTPase activity in the depolymerization of FtsZ has not been fully addressed.

† T.M.S. was funded by the European Commission Framework IV.

* To whom correspondence should be addressed: E-mail Thomas_M_Sossong@sbphrd.com or kp95955@glaxowellcome.com.

‡ Department of Anti-Infectives Research.

§ Department of Structural Biology.

|| Present address: Protein Chemistry Group, Central Research, Pfizer, Inc., Eastern Point Rd., Groton, CT 06340.

⊥ Present address: Department of Molecular Sciences, Glaxo-Wellcome Inc., 5 Moore Dr., P.O. Box 13398, Research Triangle Park, NC 27709-3398.

10.1021/bi990917e CCC: $18.00
Published on Web 10/21/1999

Here, we provide evidence that FtsZ self-activates its GTPase activity by oligomerization and we address the solution state of the enzyme in the presence of nucleotide and metal ion. Further, we have sought to fully characterize the enzymatic activity of *Escherichia coli* FtsZ using a real-time fluorescence assay. These studies directly contribute to our understanding of the molecular properties of this essential bacterial cell cycle protein.

EXPERIMENTAL PROCEDURES

Enzyme Preparation. The clone for overexpression of *E. coli* FtsZ was a gift from Dr. Miguel Vicente (Centro de Investigaciones Biológicas, Madrid). Enzyme was expressed in BL21(DE3) cells with 1 mM IPTG.[1] After 2 h of induction, cells were harvested and frozen at −80 °C. Thawed cell pellets were resuspended in 50 mM Tris, pH 7.5, 0.1 mM EDTA, and 10% glycerol to a final volume of 5 mL/g wet cell paste. Protease inhibitors (PMSF and benzamidine) were added to 1 mM final concentration and then lysozyme was added to 0.5 mg/mL. After lysis and brief sonication, cell debris was removed by centrifugation at 20000*g* for 30 min. FtsZ was precipitated from the resulting protein solution with 25% ammonium sulfate and then dialyzed against resuspension buffer. The solution was then applied to a DEAE-Sepharose column in resuspension buffer. Protein was eluted with a gradient from 0 to 900 mM KCl and fractions containing FtsZ were pooled and desalted into resuspension buffer. The partially purified FtsZ was then bound to a Pharmacia Mono P column run as an anion exchanger and eluted with a gradient from 0 to 900 mM KCl. This polishing step removed both low and high molecular weight contaminants from the DEAE-purified enzyme. Fractions containing >95% pure FtsZ as judged by SDS−PAGE were pooled. Pure enzyme was flash-frozen in liquid nitrogen and stored at −80 °C. FtsZ concentration was measured with the Pierce Coomassie blue dye binding assay, standardized by amino acid analysis.

Purified FtsZ was found to contain 0.5 GDP/subunit. Nucleotide content was determined by measuring the A_{260} of the supernatant resulting from a 3% perchloric acid precipitation of FtsZ. The identity of the bound nucleotide was determined by analysis of a sample of the supernatant on a Pharmacia Mono Q ion-exchange column and comparing the elution profile with GDP and GTP standards.

FtsZ Mutagenesis. Site-directed mutagenesis of FtsZ was carried out with the Stratagene Quick-Change mutagenesis kit. Primers were designed and PCR reactions were conducted as per Stratagene instructions. Mutations were confirmed by dsDNA sequencing on a model 377 Fluorescence Sequencing Unit (PE Biosystems) with a Taq dye terminator. Primers to the T7 promoter/terminator regions were used for sequencing reactions. Expression and purification of R214A and R214K FtsZ was the same as for wild-type FtsZ.

Kinetic Assays. GTPase activity of FtsZ was monitored by a fluorometric coupled assay (*15*). This method monitors phosphate production in real time, using phosphate from GTP hydrolysis to convert 7-methylguanosine (MEG) to 7-methylguanine (7MG) and ribose 1-phosphate. 7MG has a much lower quantum yield than MEG, resulting in a decrease in fluorescence. Standard curves generated with known phosphate concentrations were used to directly determine phosphate production from GTP hydrolysis. A typical assay contained 5 μM FtsZ, 200 μM MEG, 0.2 unit/mL nucleoside phosphorylase, 100 mM KCl, and 50 mM HEPES, pH 7.5. The assay was started with addition of GTP, and GTP concentrations were varied between 20 and 250 μM. Assays were conducted at 37 °C unless otherwise noted and were carried out with a BMG Polarstar fluorescence plate reader. High rates of phosphate production were confirmed by a colorimetric phosphate detection assay based on malachite green (*16*). Experiments varying FtsZ concentration were performed under similar conditions, except that a fixed GTP concentration of 500 μM was used. k_{cat} values were calculated from the total FtsZ concentration in the assay.

Circular Dichroism of FtsZ. FtsZ circular dichroism (CD) experiments were conducted on a Jasco 710 spectropolarimeter. Prior to an experiment, enzyme was buffer-exchanged into 5 mM phosphate, pH 7.4, by use of a desalting column. Experiments were conducted in dialysis buffer at 20 °C. Spectral analyses were performed with the Jfit program (Dr. Bernhard Rupp, http://www-structure.llnl.gov).

Analytical Ultracentrifugation of FtsZ. Sedimentation equilibrium analytical ultracentrifugation of FtsZ was carried out on a Beckman XL-I analytical ultracentrifuge. Because *E. coli* FtsZ contains no tryptophan residues, and because some experiments were conducted in the presence of high concentrations of nucleotides, interference optics (675 nm) were used to measure the concentration of FtsZ (1 mg/mL FtsZ = 3.3 fringes). Enzyme was prepared for ultracentrifugation by exhaustive dialysis into the desired experimental buffer. This dialysis removed all residual nucleotide in the enzyme preparation. Samples were prepared in 50 mM HEPES, pH 7.5, with 100 mM KCl, and FtsZ concentrations ranged from 0.5 to 1 mg/mL. The centrifuge was run at 18 000 rpm, 10 °C (except where indicated), and data were collected over a 40-h period. Data were collected at 4-h intervals and equilibrium was determined by observing that no difference appeared in the exponential distribution data between two instances of data acquisition. Equilibrium data was analyzed with software written with IGOR (WaveMetrics, Lake Oswego, OR). A partial specific volume of 0.740 and an effective molar extinction coefficient of 134 716 fringes M^{-1} cm^{-1} was used for FtsZ calculations.

FtsZ Cross-Linking. Cross-linking experiments were performed with the homobifunctional reagent dimethyl pimelimidate (Sigma). For all samples, cross-linker was added at 500:1 molar ratio to FtsZ and the reaction was allowed to proceed for 30 min in 50 mM HEPES, pH 8.0. Perchloric acid was added to 5% to stop the reaction and precipitate FtsZ. Protein was pelleted by centrifugation and then resuspended by boiling in SDS−PAGE sample buffer. Samples (approximately 0.2 μg each) were electrophoresed on SDS−4−12% polyacrylamide gels and transferred to poly(vinylidene difluoride) membranes (Novex). Membranes were probed with rabbit anti-FtsZ antisera (1:5000; a gift of M. Inouye, Robert Woods Medical Institute) and donkey anti-rabbit HRP conjugate (1:5000; Amersham). The western

[1] Abbreviations: wt, wild type; IPTG, isopropyl β-D-thiogalactopyranoside; PMSF, phenylmethanesulfonyl fluoride; MEG, 7-methylguanosine; 7MG, 7-methylguanine; CD, circular dichroism; AUC, analytical ultracentrifugation.

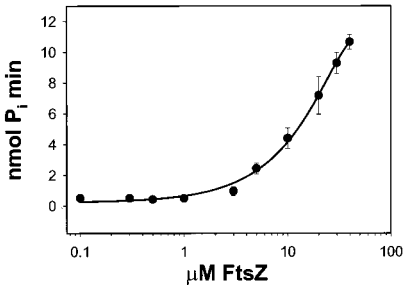

FIGURE 1: Concentration dependence of *E. coli* FtsZ GTPase activity. Phosphate production was monitored by a real-time fluorescence-based assay, with 200 μM GTP, at 37 °C. The GTPase activity of FtsZ displays a nonlinear dependence on the concentration of FtsZ. GTPase activity was not detectable below 2 μM enzyme.

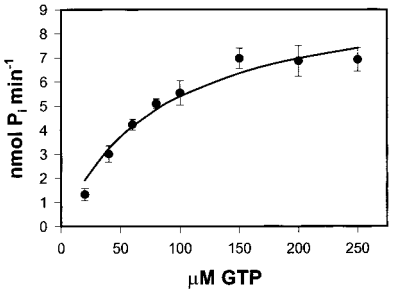

FIGURE 2: Michaelis−Menten kinetics of *E. coli* FtsZ. By use of a real-time fluorescence-based assay to monitor phosphate production, the GTPase activity of FtsZ was characterized with 5 μM enzyme at 37 °C. The K_M was determined to be 82 μM GTP and the V_{max} was 490 nmol of P_i min^{-1} mg^{-1}.

blots were developed using the Amersham ECL method, and exposed films were scanned and analyzed by densitometry (Molecular Dynamics, ImageQuant software).

RESULTS

GTPase Activity of FtsZ Monitored by a Real-Time Fluorescence Assay for Phosphate Release. The GTPase activity of wild-type *E. coli* FtsZ was evaluated by monitoring phosphate release with a fluorometric coupled assay, using nucleoside phosphorylase and 7-methylguanosine (MEG) (*15*). Unlike most enzymes, the GTPase activity of FtsZ demonstrated a nonlinear dependence on FtsZ concentration (Figure 1). Below 1 μM FtsZ, no GTPase activity could be detected. GTP hydrolysis was monitored at various GTP concentrations from 20 to 250 μM. Using Michaelis−Menten analysis, we determined a $K_M = 82$ μM GTP and $V_{max} = 490$ nmol of P_i min^{-1} (mg of protein)$^{-1}$ (Figure 2). The rate of GTPase activity was unchanged between pH 7.0 and 8.0. We found that the GTPase activity of FtsZ did not change significantly between 20 and 37 °C but that more precise results were obtained at the higher temperature. At 20 °C, the K_M dropped by 25% and the V_{max} by 30%. However, the minimal concentration required for enzymatic activity (about 1 μM) did not significantly change with this temperature difference.

We observed neither a lag nor a burst of activity in the initial rate phase of our progress curves, and the reaction rapidly went to completion even with 10 μM FtsZ and 2 mM GTP. This is in contrast to tubulin behavior, where a biphasic GTPase activity is seen as polymer formation reaches steady state in solution (*17*). The most likely explanation for this difference is that under our conditions stable FtsZ polymers are not formed in solution. However, we cannot discount the possibility that FtsZ polymers may also exchange and hydrolyze GTP.

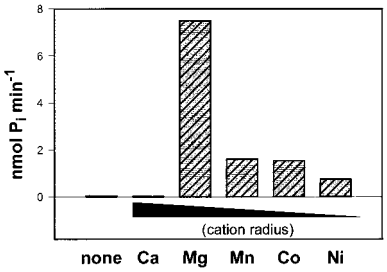

FIGURE 3: Effect of divalent metals on FtsZ GTPase activity. By use of the fluorescence-based phosphate assay, the effect of 5 mM divalent cation on the FtsZ GTPase activity was determined. Each assay contained 200 μM FtsZ and was conducted at 37 °C.

Using the real-time phosphate release assay, we evaluated the metal ion specificity for the GTPase activity of FtsZ. Figure 3 illustrates the strict requirement that *E. coli* FtsZ has for Mg^{2+}. While Mn^{2+} and Co^{2+} can weakly substitute for Mg^{2+}, the enzyme requires Mg^{2+} for full catalytic activity. Ca^{2+} has been shown to induce polymerization of FtsZ (at $[Ca^{2+}] \sim 10$ mM) and enhance the GTPase activity when included with Mg^{2+} (at $[Ca^{2+}] < 2.5$ mM) (*12*). However, we have shown that Ca^{2+} cannot provide FtsZ with any GTPase activity when used as the sole divalent cation.

Distribution of FtsZ Oligomer Species by Sedimentation Equilibrium Analytical Ultracentrifugation. To gain insights on the solution properties of FtsZ, we used sedimentation equilibrium analytical ultracentrifugation (AUC). At thermodynamic equilibrium, molecules will be dispersed as an exponential and this distribution data contains information about the quaternary state of the sample (*18*). For molecules with dissociation constants between 10^{-3} and 10^{-8}, oligomeric state(s) can be determined, thus providing information about the concentration of particular species.

Using this approach, we show that, in the absence of nucleotides, FtsZ exists in oligomeric states beyond monomer (Figure 4). These AUC experiments revealed both dimeric and trimeric species in addition to monomeric FtsZ. Calculated equilibrium constants are $K_{1,2} = 0.15 \pm 0.03$ μM and $K_{2,3} = 2.7 \pm 0.26$ μM (Table 1). We found no difference in the AUC results when FtsZ was examined in the presence of NaCl or KCl. We also found that there was a small temperature dependence for the FtsZ self-association, with the $K_{1,2}$ increasing to 0.57 μM when the temperature was increased to 18 °C. These findings provide the first evidence that FtsZ can exist in discrete oligomeric states in the absence of nucleotide, metals, and other cell division components.

Effect of Nucleotides and Metal Ions on FtsZ Subunit Association. AUC was used to determine the effect of guanine nucleotides and analogues on the association of FtsZ subunits. Because the combination of GTP and Mg^{2+} results in rapid hydrolysis of the nucleotide, we considered nonhydrolyzable GTP analogues. However, we found that nonhydrolyzable GTP analogues β,γ-methyleneguanosine 5′-triphosphate and β,γ-imidoguanosine 5′-triphosphate do not compete activity in a typical GTPase assay (data not shown). In the absence of AUC data with GTP + Mg^{2+}, we conducted experiments in the presence of GDP, GTP, without

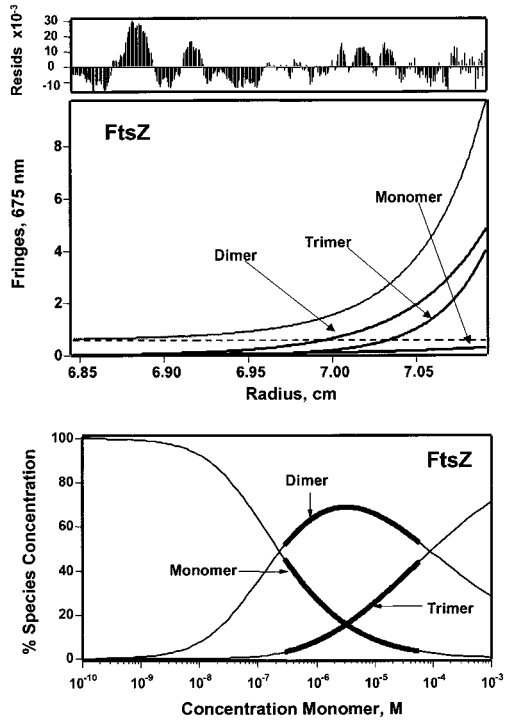

FIGURE 4: Analytical ultracentrifugation (AUC) analysis of wild-type FtsZ. In solution, and in the absence of nucleotide or metal, FtsZ can exist in several discrete oligomeric states, including monomer, dimer, and trimer. Analysis was performed with 1 mg/mL enzyme at 10 °C, pH 7.5. The dotted line in the upper panel indicates the fit of the exponential distribution data. The thicker portions of the curves in the lower panel indicates the range of data obtained directly from sample.

Table 1: Thermodynamic Constants for *E. coli* FtsZ Oligomerization Determined by Analytical Ultracentrifugation[a]

FtsZ	ligand	$K_{1,2}$ (μM)	$K_{2,3}$ (μM)
wild type	none	0.15 ± 0.03	2.7 ± 0.26
wild type	GDP (1mM)	31 ± 0.90	31 ± 0.55

[a] Protein distribution data from equilibrium AUC experiments were most appropriately analyzed with a monomer−dimer−trimer fitting analysis. Constants were determined directly from the fits (*18*).

Mg^{2+}, Mg^{2+}, and GDP + Mg^{2+}. Mechanistically, it has been suggested that GDP plays a role in destabilization of FtsZ polymers in vitro (*11*). Using AUC, we found that 1 mM GDP significantly shifts the monomer−dimer equilibrium to higher FtsZ concentrations with a calculated $K_{1,2} = 31 \pm 0.9$ μM and $K_{2,3} = 31 \pm 0.55$ μM (Figure 5, top, and Tables 1 and 2). GTP strongly stabilized the formation of tetrameric FtsZ, a larger oligomeric species not found with FtsZ alone, but slightly increased the concentration at which dimeric FtsZ is first observed (Figure 5, bottom, and Table 2). As FtsZ concentration increases, the percentage of tetrameric species also increases. Table 2 shows the different effect of bound GTP versus bound GDP on 2 μM FtsZ, implicating the two nucleotides in two different roles. GTP stabilizes higher order oligomer formation, while GDP destabilizes oligomeric FtsZ and stabilizes the monomeric state. Interestingly, 5 mM Mg^{2+} caused an increase in trimer/tetramer formation (Figure 6, top, and Table 2). In the presence of GDP, this Mg^{2+}-mediated increase was very similar (Figure 6, bottom, and Table 2). The Mg^{2+}-based changes in the association of FtsZ were best fit to a monomer−dimer−trimer−tetramer model.

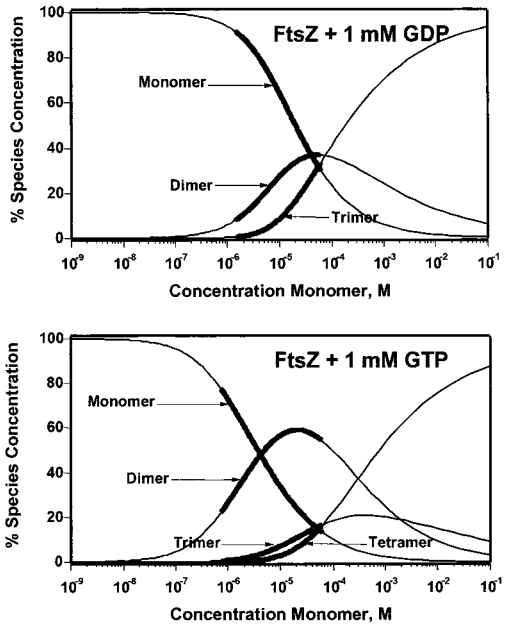

FIGURE 5: AUC plots for FtsZ with GDP and GTP. (Top) FtsZ in the presence of 1 mM GDP. (Bottom) FtsZ in the presence of 1 mM GTP (no Mg^{2+}).

Table 2: Percentage Distribution of FtsZ Oligomeric Species at 2 μM FtsZ[a]

	monomer	dimer	trimer	tetramer
no ligand	19	68	13	0
GDP	89	5	1	0
GTP (no Mg^{2+})	58	38	3	1
Mg^{2+}	33	64	2	1
Mg^{2+} + GDP	38	57	3	2

[a] Nucleotides were used at 1 mM and $MgCl_2$ was present at 5 mM. AUC experiments were conducted and analyzed as described under Experimental Procedures.

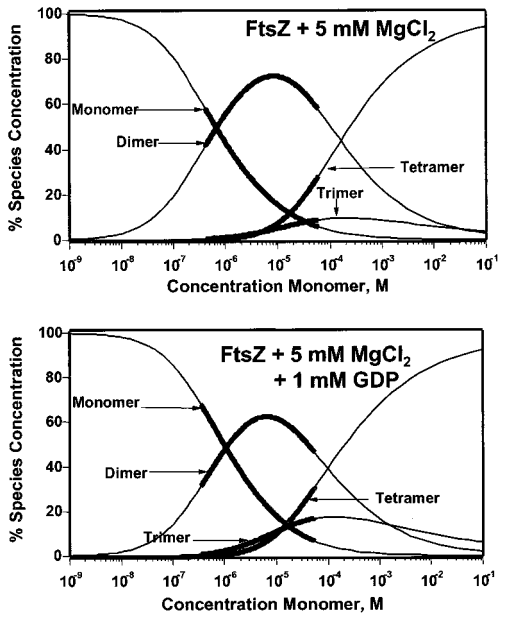

FIGURE 6: AUC plots for FtsZ with Mg^{2+}. (Top) FtsZ in the presence of 5 mM $MgCl_2$. (Bottom) FtsZ in the presence of 5 mM $MgCl_2$ and 1 mM GDP.

Addition of 5 mM Ca^{2+} to FtsZ showed a stabilization of dimeric and tetrameric FtsZ oligomers (data not shown). Additionally, there is a lower apparent protein concentration

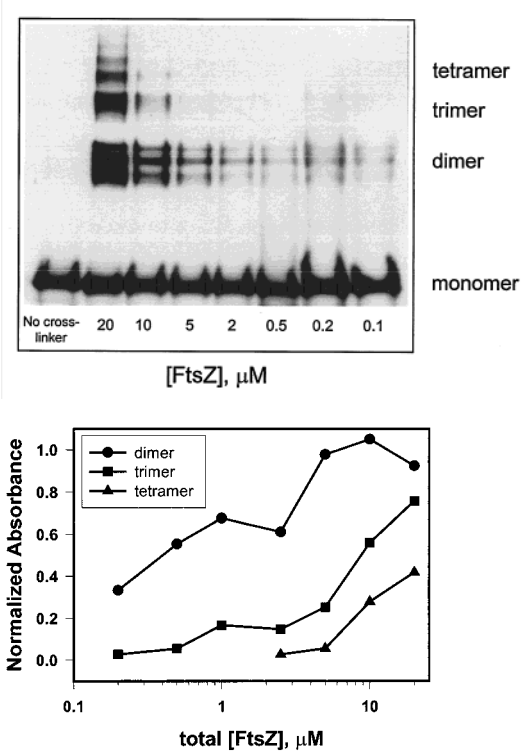

FIGURE 7: Chemical cross-linking of FtsZ. (Top) Various concentrations of *E. coli* FtsZ were incubated with dimethyl pimelimidate at a 500-fold molar excess. Samples were electrophoresed and western-blotted, and FtsZ was detected by the ECL method (see Materials and Methods). (Bottom) Exposed films were analyzed by densitometry.

in these samples, indicating that some FtsZ aggregates may have been centrifuged out of solution. These preliminary experiments suggest that Ca^{2+} may have a stabilizing effect on larger FtsZ polymers.

Chemical Cross-Linking Confirms That FtsZ Is Dimeric and Trimeric in Solution. To further substantiate the AUC results, we used chemical cross-linking with dimethyl pimelimidate to identify oligomeric species of FtsZ. Cross-linking as a function of FtsZ concentration clearly shows that FtsZ is primarily monomeric below 1 μM (Figure 7, top). At higher FtsZ concentrations, dimeric, trimeric, and tetrameric species are observed. Densitometry analysis shows that both dimer and trimer species begin to appear at concentrations similar to those determined by equilibrium AUC (Figure 7, bottom).

GTPase Activity for FtsZ Mutants of a Well-Conserved Arginine Residue. Since we have shown that there is a strong correlation between appearance of FtsZ oligomers (at $\sim$1 μM) and GTPase activity, we investigated the possibility that a well-conserved arginine might play a role in GTP hydrolysis. Precedence for this exists in the Ras proteins, where a GTPase activating protein (GAP) provides an "arginine finger" that accelerates GTPase activity almost 10^5-fold (*19*). Comparison of crystal structures of FtsZ (*7*) and the $\alpha-\beta$ tubulin dimer (*8*) shows that the HC1 loop (amino acids 204−217) in *E. coli* FtsZ may be involved in a dimer interface. Additionally, nearly all residues in this loop are highly conserved among bacterial species and this further suggests that this loop plays an important functional role. Upon examination of the structural model of FtsZ, it appeared possible that the side chain of arginine 214 could point toward the GTP binding site upon FtsZ dimerization. We mutated the well-conserved R214 to both an alanine and lysine to check the possibility that this residue may function as an "arginine finger".

Table 3: Kinetic Parameters for *E. coli* FtsZ GTPase Activity[a]

FtsZ	K_m (μM)	V_{max} [nmol of P_i min^{-1} (mg of protein)$^{-1}$]	k_{cat}[b] (min^{-1})
wild type	82 ± 17	490 ± 40	19.7[c]
R214A	220 ± 78	710 ± 140	25.8

[a] Rates of GTP hydrolysis by FtsZ were monitored with 5 μM FtsZ in a real-time fluorescence assay, as described under Experimental Procedures. Rates plotted as a function of GTP concentration were nonlinear curve-fit to the Michaelis−Menten equation. [b] The turnover rate was determined by using total moles of FtsZ. [c] The k_{cat} values were 24.0 min^{-1} and 13.6 min^{-1} at 3 μM and 7.5 μM FtsZ, respectively.

Interestingly, both R214A and R214K mutations caused little change in the GTP hydrolytic activity. The enzymatic parameters for R214A, at 5 μM enzyme, were determined to be $K_M = 220 \pm 78$ μM GTP and $V_{max} = 710 \pm 140$ nmol of P_i min^{-1} (mg of protein)$^{-1}$ (Table 3). The concentration dependence of the GTPase activity of R214A was also comparable to that of wild-type FtsZ (data not shown). Therefore, we conclude that the well-conserved arginine at position 214 is not involved in catalytic enhancement via a "GAP-like" function upon FtsZ dimerization.

Circular Dichroism Shows That Mg^{2+} Induces a Structural Change in FtsZ. In enzyme function, Mg^{2+} can play both a structural and a catalytic role. For GTPases, the catalytic role of Mg^{2+} involves coordination of the β- and γ-phosphates of GTP, and this Mg^{2+} is essential for GTP hydrolysis (*20*). Similar to many GTPases, FtsZ can bind but not hydrolyze GTP in the absence of Mg^{2+} (*21*). Titration of FtsZ from 410 nM to 7.4 μM did not reveal any measurable change in the secondary structure.

Circular dichroism was used to determine whether Mg^{2+} played a structural as well as a catalytic role in FtsZ function. Titration of FtsZ with Mg^{2+} to 25 mM caused a 20% increase in α-helical content at 222 nm, from 40% to about 49% (Figure 8). This effect was saturated at approximately 2 mM Mg^{2+}. Addition of Ca^{2+} to FtsZ also yielded a structural change similar to that observed with Mg^{2+} (data not shown). However, CD spectra suggest Ca^{2+} may also influence β-sheet content. The control experiment with 50 mM K^+ showed a small ionic strength effect, but the results with Mg^{2+} and Ca^{2+} were above this background. There was no substantial difference in the CD spectra of wild-type and R214A FtsZ. Surprisingly, we found no evidence of structural changes upon addition of either GDP or GTP to wild-type enzyme.

DISCUSSION

E. coli FtsZ was first shown to specifically bind and hydrolyze GTP by de Boer et al. (*6*) and subsequently by other investigators (*21*, *22*). Using a real-time fluorescence-based phosphate assay, we have fully characterized this hydrolytic activity. Most strikingly, and similar to *Bacillus subtilis* FtsZ (*23*), *E. coli* FtsZ displays a cooperative increase in catalytic activity between 1 and 10 μM and between these concentrations GTPase activity is dramatically increased (Figure 1). However, at any one particular enzyme concentration, the rate of phosphate production is linear and does

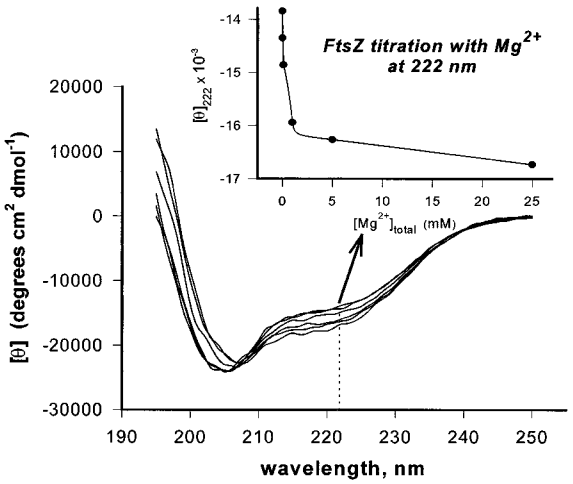

FIGURE 8: Effect of Mg^{2+} on the secondary structure of FtsZ. A titration from 0 to 25 mM $MgCl_2$ (0, 0.01, 0.1, 1, 5, and 25 mM) induces a structural change in FtsZ, most notably in the α-helical content of the enzyme. The experiment was run at 20 °C in 5 mM sodium phosphate, pH 7.4. A control experiment containing 50 mM KCl induced only a minimal change in secondary structure and with a different overall spectrum shape.

not exhibit a burst or lag in activity. Below 1 μM FtsZ concentration no GTP hydrolytic activity is detectable; this limit is not due to the sensitivity of our fluorescence-based assay, as picomolar levels of phosphate are readily detectable. The strong concentration dependence of FtsZ GTPase activity suggests that a self-association event is responsible for "switching on" the enzyme's activity.

At 5 μM FtsZ, we determined a K_M for GTP of 82 μM and a V_{max} of 490 nmol min^{-1} (mg of protein)$^{-1}$ for *E. coli* FtsZ (Figure 2). From the value for total FtsZ in solution, the k_{cat} for this reaction is 19.7 min^{-1}. Our rate measured by the real-time fluorescence assay is somewhat faster than previously reported rates (~2 min^{-1}) (*12*, *22*). Assay conditions are virtually identical for each of these measurements with the significant differences being that our assay is a real-time, nonintrusive assay that does not require radiolabeled [γ-^{32}P]GTP and that our kinetic parameters are based on a traditional kinetic analyses. Interestingly, the rate of GTP hydrolysis for *E. coli* FtsZ is significantly faster than that for tubulin oligomers (0.2 μM min^{-1} vs 4.9 μM min^{-1} for FtsZ in this study; *27*). However, direct comparison of FtsZ and tubulin rates is difficult because we were unable to establish a reliable time-resolved assembly assay for *E. coli* FtsZ and thus could not characterize rates for both free and polymer-incorporated FtsZ. One possible source of this difficulty is that FtsZ polymers are relatively short-lived and unstable compared to tubulin microtubules. Again, it is with caution that the GTPase activity of FtsZ is compared with that of tubulin. Tubulin polymerizes as a heterodimer, only one subunit of the heterodimer can hydrolyze GTP, and the nucleotide bound between two tubulin subunits is nonexchangeable. In the case of FtsZ, every subunit is identical, and as such, every subunit interface will likely hydrolyze GTP. Because of the transient nature of the FtsZ polymer, it is not currently known whether polymer-bound nucleotide is exchangeable.

An additional characteristic of tubulin GTPase activity is that at critical concentrations, GTP hydrolysis undergoes a rapid burst followed by a slower, linear hydrolysis that occurs as microtubule assembly reaches steady state (*24*, *25*). We observed no evidence of this process with the FtsZ GTPase reaction (data not shown). This result again suggests that FtsZ polymers are intrinsically more dynamic in vitro than tubulin microtubules. On the basis of other reports (*12*, *26*), the conditions of our enzymatic assay are "nonpolymerizing" conditions. That is, in our system, we are not examining the formation of very large, long-lived polymers of FtsZ but more likely intermediate-length, transient linear oligomers. This stage is similar to the linear polymerization phase observed for microtubule assembly (*27*).

Typically, to observe polymers and larger sheetlike assemblies of FtsZ in vitro, stabilizing agents such as Ca^{2+}, DEAE-dextran, and cationic lipid substrates are required. Like Yu and Margolin (*12*), we have found that the GTP hydrolysis rate of *E. coli* FtsZ is dramatically decreased with 10 mM Ca^{2+} (data not shown). At 5 mM Ca^{2+}, preliminary AUC experiments have shown that a significant amount of protein is lost from solution during the 24 h run. This suggests that Ca^{2+} stabilizes large polymers of FtsZ, similar to the results reported by Yu and Margolin (*12*). We conclude that this concentration of Ca^{2+} induces polymer formation and this may be related to the decreased rate of GTPase activity. One possibility is that Ca^{2+} can displace Mg^{2+}, perhaps at the subunit interface, thus slowing GTP hydrolysis and increasing polymer stability. In fact, by reverse analogy, it has been shown that tubulin mutants with increased rates of GTP hydrolysis also have increased microtubule dynamic instability (*25*). However, its remains unclear whether the Ca^{2+} effect on FtsZ is specific or simply a nonspecific, charge-shielding effect.

In general, we assume that our solution conditions, for both GTPase and AUC experiments, allow us to observe activities during the linear assembly phase, somewhat analogous to the prenucleation phase in tubulin assembly (*27*). It is not currently known if FtsZ polymerizes to any significant extent in vivo through lateral contacts. Published data indicate that DEAE-dextran can act as a support and stabilize FtsZ in three-dimensional "sheets" (*14*, *28*). Furthermore, in vivo fluorescence microscopy studies with GFP-FtsZ show that FtsZ does indeed assemble into a ring structure at the division site (*3*, *4*). It is not known from the current resolution if the FtsZ ring is of single or several subunit lateral thickness, but it can be concluded that the FtsZ ring does not form a wide sheetlike structure at the midcell. This conclusion is supported by the fact that the copy number of FtsZ in the cell (15 000−20 000) would allow a complete FtsZ ring to circle the midcell no more than a few times.

Because of the strong concentration dependence of FtsZ GTPase activity (and oligomer formation; see below), we conducted GTPase assays at several FtsZ concentrations (Table 3). k_{cat}, calculated from the total moles of FtsZ, decreases as enzyme concentration increases (from 24 to 13.6 min^{-1} as FtsZ concentration increases from 3 to 7.5 μM). K_M also decreases with increasing enzyme concentration but to a greater extent than does the k_{cat}. As a result, the k_{cat}/K_M ratio (apparent second-order rate constant in Michaelis−Menten kinetics) for FtsZ GTPase activity decreases with increasing enzyme concentration. We explain this as follows: AUC and cross-linking show that oligomeric forms of FtsZ become more prevalent as the enzyme concentration

is increased. If nucleotide cannot diffuse into and out of *polymerized* FtsZ (as is the case in tubulin polymers), the prevalence of FtsZ oligomers at higher enzyme concentrations effectively decreases the number of available "active sites" for GTPase activity. As enzyme concentration increases, the equilibrium for FtsZ subunit association is shifted to the right, slowing the overall turnover of FtsZ subunits from oligomer to monomer. GTP hydrolysis by FtsZ basically follows Michaelis−Menten kinetics but does not strictly follow this model. k_{cat}/K_M generally sets the lower limit for the rate constant describing association of enzyme and substrate in an enzymatic reaction, but in the case of FtsZ GTPase activity, k_{cat}/K_M may reflect the rate for enzyme subunit association.

Due to some of the interesting differences between FtsZ and tubulin GTP hydrolysis, we wished to further investigate the solution properties of FtsZ by analytical ultracentrifugation (AUC). The intention of these experiments was to gain insights into molecular properties that govern GTP hydrolysis. AUC experiments in the absence of metal ions and nucleotide clearly show that FtsZ can self-associate (Figure 4). On the basis of the goodness of the curve-fit residuals and consistent χ^2 values, an analysis describing a monomer−dimer−trimer equilibrium was judged the best fit. By this analysis, the equilibrium constants for monomer to dimer and dimer to trimer are 0.15 and 2.7 μM, respectively. These results show for the first time that FtsZ can exist in discrete oligomeric states in solution, in the absence of nucleotide.

A comparison of the AUC results with FtsZ GTPase properties reveals that at enzyme concentrations where monomeric enzyme dominates, hydrolytic activity cannot be observed. This conclusion is further supported by the cross-linking results, which also indicate the absence of oligomeric FtsZ at low protein concentrations. We conducted AUC experiments at two temperatures (10 and 18 °C) and we observed a small increase in the $K_{1,2}$ for FtsZ from 0.15 to 0.57 μM, respectively. In a similar trend, the maximal rate of GTP hydrolysis by FtsZ increases as the temperature is increased from 20 to 37 °C (30% increase). This change is actually smaller than one might estimate on the basis of the Arrhenius equation, although this relationship is not expected to apply since FtsZ GTPase activation is complicated by an association step. Interestingly, the concentration dependence profile of FtsZ GTPase activity does not significantly change between 20 and 37 °C where GTPase activity is only observed starting at about 1 μM FtsZ (data not shown).

GDP markedly shifts the monomer−dimer equilibrium of FtsZ from 0.15 to 31 μM (Figure 5, top, and Table 1). These AUC results suggest that FtsZ with GDP bound may exist in a different conformation than FtsZ in the absence of nucleotide, although we could not detect a structural difference by CD. The fact that GDP-bound FtsZ exists as monomer suggests a "depolymerizing" role for (bound) GDP after GTP hydrolysis. Such a duality of function for bound nucleotide supports the dynamic nature of the FtsZ ring in vivo. In the presence of GTP, tetrameric FtsZ species are seen at high FtsZ concentrations (>2 μM) (Figure 5, bottom, and Table 2). Interestingly, these results show that in the absence of stabilizing agents such as DEAE dextran the "polymerizing" effect of GTP alone is not dramatic, consistent with a previous report by Mukherjee and Lutkenhaus (*11*). It is likely that both GTP and Mg^{2+} are required for polymer assembly. Unfortunately, because sedimentation equilibrium AUC runs require >24 h, experiments with both Mg^{2+} and GTP are not possible due to GTP hydrolysis by FtsZ. Because FtsZ + GTP AUC data was best fit to a monomer−dimer−trimer−tetramer model, an accurate calculation of the $K_{1,2}$ equilibrium constant was not feasible. However, the noted differences between the solution behavior of FtsZ in the presence of either GTP or GDP support the idea that the FtsZ ring, like a microtubule, is dynamic in nature, with GTP/Mg^{2+} stabilizing FtsZ oligomer formation and GDP destabilizing the FtsZ polymer.

Mg^{2+} was found to slightly promote higher order FtsZ oligomer formation. In the presence of 5mM Mg^{2+}, we could clearly detect monomer, dimer, trimer, and tetramer in our AUC experiments (Figure 6). Noting this apparently "linear" addition of subunits to the FtsZ polymer, it is likely that there are higher order FtsZ oligomers (pentamer, hexamer, etc.) in solution during the AUC experiments but at concentrations too low to detect with the interference optical system. It is interesting to note that, at millimolar concentrations of Mg^{2+}, FtsZ is optimally active as a GTPase, exists in multimeric states, and undergoes a slight change in secondary structure as indicated by CD spectroscopy (Figure 8). These three phenomena clearly demonstrate the significant role that Mg^{2+} plays in FtsZ function. Even in the presence of GDP, which stabilizes the monomeric form of FtsZ, Mg^{2+} induces higher order oligomer formation (Figure 6, bottom). These results may also indicate that the structural change in FtsZ upon Mg^{2+} binding (Figure 8) exposes additional FtsZ−FtsZ binding sites and that this effect overrides the monomerizing effect of GDP alone.

The conclusion that FtsZ assembles in a linear fashion is strongly supported by chemical cross-linking experiments. Figure 7 shows that a significant portion of FtsZ in solution is in dimer form at 0.5 μM FtsZ concentration. As FtsZ concentration is increased, we find that dimer concentration increases in addition to higher order oligomers. The size of the oligomers increases with the addition of single FtsZ subunits. In lanes containing the 5 μM, 10 μM, and 20 μM samples, a ladderlike effect is observed. It is very interesting to note that the oligomer formation appears somewhat exponential, much like that seen with the concentration dependence on GTPase activity (Figure 1). This result again strongly suggests that FtsZ subunit assembly is required for triggering of GTPase activity.

With some GTPases, such as $p21^{ras}$, the GTPase activity is insignificant when catalyzed by the enzyme alone. When the *ras* GTPase activating protein or GAP interacts with $p21^{ras}$, the ras GTPase activity is enhanced several orders of magnitude (*29*). The GAP-mediated stimulation of $p21^{ras}$ activity occurs by way of a critical arginine residue termed the "arginine finger" (*19*). This arginine fits perfectly into the GTP binding site of $p21^{ras}$ and enhances catalysis by stabilizing the transition state of the GTPase reaction (*19*). In the case of *E. coli* FtsZ, there is an arginine residue, R214, that is found in the small helix following the "synergy loop". In FtsZ from other organisms, the positive charge at this position is highly conserved as an arginine or lysine.

As suggested by comparison of the FtsZ structure with the structure of the tubulin dimer, R214 from one monomer subunit may be able to participate in hydrolysis at the active

site in an adjoining monomer subunit, much like the "arginine finger" functions in the p21^{ras}−GAP complex. To test this hypothesis, we made two mutations at R214. A mutation to alanine was designed to abolish any possible participation of R214 in catalysis, and R214K was designed to conserve any possible catalytic participation of R214. Both R214A and R214K have activities very similar to that of wild-type FtsZ (Table 3), illustrating that R214 does not directly participate in GTP hydrolysis. Additionally, the CD spectrum of R214A is nearly identical to that of wild-type FtsZ, showing that this mutation does not disrupt the secondary structure. Also, the AUC results show that R214A FtsZ can oligomerize in the same pattern as wild-type FtsZ, ruling out that R214 participates in FtsZ−FtsZ subunit interactions.

Using a combination of enzymatic and solution structural techniques, we have identified a "GTPase switch" in *E. coli* FtsZ. We have conclusively shown that GTPase activity of FtsZ occurs at a concentration where we observe oligomeric species. Our data suggest that FtsZ must at least dimerize (and possibly trimerize) to become an active GTPase. In this model, GTP most likely resides between two FtsZ subunits, which then constitute a shared active site that may aid polymer formation. Unlike tubulin polymer assembly by dimers, our solution data suggest that monomers of FtsZ are the fundamental building blocks for polymer formation. Mutagenesis efforts will be required to more specifically define both catalytic residues in the GTP active site and residues that are responsible for subunit association. Such studies are crucial for further understanding the precise role that GTP binding and hydrolysis play in regulating the FtsZ polymerization−depolymerization cycle.

ACKNOWLEDGMENT

We thank Dr. Michael L. Doyle for his assistance with the CD spectroscopy, the SmithKline Beecham U.S. DNA sequencing facility for their work, and Dr. Miguel Vicente for his generous gift of the *E. coli* FtsZ cDNA.

REFERENCES

1. Lutkenhaus, J., and Addinall, S. G. (1997) *Annu. Rev. Biochem. 66*, 93−116.
2. Bi, E. F., and Lutkenhaus, J. (1991) *Nature 354*, 161−164.
3. Ma, X., Ehrhardt, D. W., and Margolin, W. (1996) *Proc. Natl. Acad. Sci. U.S.A. 93*, 12998−13003.
4. Sun, Q., and Margolin, W. (1998) *J. Bacteriol. 180*, 2050−2056.
5. de Pereda, J. M., Leynadier, D., Evangelio, J. A., Chacon, P., and Andreu, J. M. (1996) *Biochemistry 35*, 14203−14215.
6. de Boer, P., Crossley, R., and Rothfield, L. (1992) *Nature 359*, 254−256.
7. Lowe, J., and Amos, L. A. (1998) *Nature 391*, 203−206.
8. Nogales, E., Wolf, S. G., and Downing, K. H. (1998) *Nature 391*, 199−203.
9. Bi, E., and Lutkenhaus, J. (1992) *J. Bacteriol. 174*, 5414−5423.
10. Dai, K., Mukherjee, A., Xu, Y., and Lutkenhaus, J. (1994) *J. Bacteriol. 176*, 130−136.
11. Mukherjee, A., and Lutkenhaus, J. (1998) *EMBO J. 17*, 462−469.
12. Yu, X. C., and Margolin, W. (1997) *EMBO J. 16*, 5455−5463.
13. Mukherjee, A., and Lutkenhaus, J. (1994) *J. Bacteriol. 176*, 2754−2758.
14. Erickson, H. P., Taylor, D. W., Taylor, K. A., and Bramhill, D. (1996) *Proc. Natl. Acad. Sci. U.S.A. 93*, 519−523.
15. Banik, U., and Roy, S. (1990) *Biochem. J. 266*, 611−614.
16. Lanzetta, P. A., Alvarez, L. J., Reinach, P. S., and Candia, O. A. (1979) *Anal. Biochem. 100*, 95−97.
17. Davis, A., Sage, C. R., Wilson, L., and Farrell, K. W. (1993) *Biochemistry 32*, 8823−8835.
18. Hensley, P. (1996) *Structure 4*, 367−373.
19. Ahmadian, M. R., Stege, P., Scheffzek, K., and Wittinghofer, A. (1997) *Nat. Struct. Biol. 4*, 686−689.
20. Bourne, H. R., Sanders, D. A., and Mccormick, F. (1991) *Nature 349*, 117−127.
21. Mukherjee, A., Dai, K., and Lutkenhaus, J. (1993) *Proc. Natl. Acad. Sci. U.S.A. 90*, 1053−1057.
22. RayChaudhuri, D., and Park, J. T. (1992) *Nature 359*, 251−254.
23. Wang, X., and Lutkenhaus, J. (1993) *Mol. Microbiol. 9*, 435−442.
24. Carlier, M. F., and Pantaloni, D. (1983) *Biochemistry 22*, 4814−4822.
25. Davis, A., Sage, C. R., Dougherty, C. A., and Farrell, K. W. (1994) *Science 264*, 839−842.
26. Bramhill, D., and Thompson, C. M. (1994) *Proc. Natl. Acad. Sci. U.S.A. 91*, 5813−5817.
27. Carlier, M. F., Didry, D., and Pantaloni, D. (1997) *Biophys. J. 73*, 418−427.
28. Lu, C., Stricker, J., and Erickson, H. P. (1998) *Cell Motil. Cytoskeleton 40*, 71−86.
29. Mittal, R., Ahmadian, M. R., Goody, R. S., and Wittinghofer, A. (1996) *Science 273*, 115−117.

BI990917E